NLRP3 mutation and cochlear autoinflammation cause syndromic and nonsyndromic hearing loss DFNA34 responsive to anakinra therapy

Hiroshi Nakanishi[a], Yoshiyuki Kawashima[a], Kiyoto Kurima[a], Jae Jin Chae[b], Astin M. Ross[a], Gineth Pinto-Patarroyo[b], Seema K. Patel[c], Julie A. Muskett[a], Jessica S. Ratay[a], Parna Chattaraj[a], Yong Hwan Park[b], Sriharsha Grevich[d], Carmen C. Brewer[a], Michael Hoa[e], H. Jeffrey Kim[a], John A. Butman[f], Lori Broderick[d], Hal M. Hoffman[d], Ivona Aksentijevich[b], Daniel L. Kastner[b,1], Raphaela Goldbach-Mansky[g], and Andrew J. Griffith[a,1]

[a]Otolaryngology Branch, National Institute on Deafness and Other Communication Disorders, National Institutes of Health, Bethesda, MD 20892; [b]Inflammatory Disease Section, National Human Genome Research Institute, National Institutes of Health, Bethesda, MD 20892; [c]Rheumatology Fellowship and Training Branch, National Institute of Arthritis and Musculoskeletal and Skin Diseases, National Institutes of Health, Bethesda, MD 20892; [d]Rady Children's Hospital and Department of Pediatrics, University of California, San Diego, La Jolla, CA 92093; [e]Office of the Clinical Director, National Institute on Deafness and Other Communication Disorders, National Institutes of Health, Bethesda, MD 20892; [f]Radiology and Imaging Sciences, Clinical Center, National Institutes of Health, Bethesda, MD 20892; and [g]Translational Autoinflammatory Disease Studies, National Institute of Allergy and Infectious Diseases, National Institutes of Health, Bethesda, MD 20892

The NLRP3 inflammasome is an intracellular innate immune sensor that is expressed in immune cells, including monocytes and macrophages. Activation of the NLRP3 inflammasome leads to IL-1β secretion. Gain-of-function mutations of *NLRP3* result in abnormal activation of the NLRP3 inflammasome, and cause the autosomal dominant systemic autoinflammatory disease spectrum, termed cryopyrin-associated periodic syndromes (CAPS). Here, we show that a missense mutation, p.Arg918Gln (c.2753G > A), of *NLRP3* causes autosomal-dominant sensorineural hearing loss in two unrelated families. In family LMG446, hearing loss is accompanied by autoinflammatory signs and symptoms without serologic evidence of inflammation as part of an atypical CAPS phenotype and was reversed or improved by IL-1β blockade therapy. In family LMG113, hearing loss segregates without any other target-organ manifestations of CAPS. This observation led us to explore the possibility that resident macrophage/monocyte-like cells in the cochlea can mediate local autoinflammation via activation of the NLRP3 inflammasome. The NLRP3 inflammasome can indeed be activated in resident macrophage/monocyte-like cells in the mouse cochlea, resulting in secretion of IL-1β. This pathway could underlie treatable sensorineural hearing loss in DFNA34, CAPS, and possibly in a wide variety of hearing-loss disorders, such as sudden sensorineural hearing loss and Meniere's disease that are elicited by pathogens and processes that stimulate innate immune responses within the cochlea.

cochlea | cryopyrin-associated periodic syndromes | inflammation | hearing loss | interleukin-1β

The *NLRP3* gene (NLR family, pyrin domain containing three; initially known as *CIAS1*, MIM 606416) encodes the NLRP3 protein (also referred to as NALP3 or cryopyrin), a key and eponymous component of the NLRP3 inflammasome (1). The NLRP3 inflammasome is an intracellular innate immune sensor that is expressed in immune cells, including monocytes, macrophages, and dendritic cells (2–4). NLRP3 consists of an N-terminal pyrin (PYD) domain, a central nucleotide-binding oligomerization (NACHT) domain, followed by a leucine-rich repeat (LRR) domain at the C terminus (5). When the NLRP3 inflammasome is activated, the PYD domain mediates recruitment of an adaptor protein called ASC (apoptosis-associated speck-like protein containing CARD) and the effector protein procaspase-1 to form an NLRP3 inflammasome complex that can cleave inactive procaspase-1 to form active caspase-1 (Fig. S1). Active caspase-1 can process pro–IL-1β to mature IL-1β, a potent secreted proinflammatory cytokine (1, 6, 7). Activation of the NLRP3 inflammasome is tightly regulated and requires at least two signals (8). Initial priming signals include Toll-like receptor ligands, such as bacterial lipopolysaccharide (LPS) that

lead to increased NLRP3 and pro–IL-1β mRNA and protein expression (3). The second signal can be one of a broad variety of activators such as crystalline molecules, pore-forming toxins, adenosine triphosphate (ATP), or extracellular calcium (9, 10).

Gain-of-function mutations of *NLRP3* are the cause of a spectrum of autosomal-dominant systemic autoinflammatory diseases, termed cryopyrin-associated periodic syndromes (CAPS). CAPS include three clinical subtypes: neonatal-onset multisystem inflammatory disease (NOMID, also known as CINCA, MIM 607115), Muckle-Wells syndrome (MWS, MIM 191900), and familial cold autoinflammatory syndrome (FCAS, MIM 120100). These diseases share a number of common signs and symptoms, including recurrent fever, urticaria-like rash, headache, conjunctivitis, and arthralgia or arthritis, with differences in the severity and length of disease flares, but all display serologic evidence of

---

Significance

This study identifies a mutation in the *NLRP3* gene that causes sensorineural hearing loss in human patients. *NLRP3* encodes a protein important for innate immunity, secretion of the potent cytokine IL-1β, and inflammation. The hearing loss in three affected members of one family improved or completely resolved after treatment with IL-1β blockade therapy. This study shows that the mouse *Nlrp3* gene is expressed in immune macrophage-like cells throughout the inner ear, which can be activated to release the potent cytokine IL-1β. These observations suggest that mutations of *NLRP3* may cause hearing loss by local autoinflammation within the inner ear. This mechanism could underlie a variety of hearing-loss disorders of unknown etiology that might respond to IL-1β blockade therapy.

---

systemic inflammation. Hearing loss is characteristic of NOMID and MWS, but is rarely observed in FCAS (11, 12). Thus, some individuals and families segregate atypical phenotypes with overlapping features, although the phenotypes appear to breed true within families. A single family was recently reported to cosegregate a known MWS-associated mutation of *NLRP3* with hearing loss and variable mild inflammatory manifestations (13).

NLRP3 mutations cause CAPS by constitutive activation of the NLRP3 inflammasome, leading to increased IL-1β production (5, 14, 15). Monocytes from patients with *NLRP3* mutations only require the initial priming signal by LPS to induce IL-1β secretion, whereas wild-type control cells require a second activating signal (14). This difference can be used to evaluate the pathogenicity of *NLRP3* variants. IL-1β, the most powerful fever-inducing cytokine, activates cells by binding and signaling through IL-1 receptor type I and the IL-1 receptor accessory protein. Anakinra, a nonglycosylated recombinant version of the human IL-1 receptor antagonist, significantly improves the clinical signs and symptoms and inflammatory markers of CAPS phenotypes, including NOMID, MWS, and FCAS (16–18).

The vast majority of known *NLRP3* mutations affect the NACHT domain (domain conserved in NAIP, CIITA, HET-E, and TP1), with a few mutations affecting other regions of the gene and protein, including the LRR domain (19). There are some mutations that cause one phenotype in some families and a different phenotype in others (20). However, mutations associated with FCAS are not observed in association with NOMID. Furthermore, MWS mutations are often associated with hearing loss, which presents later in life than in NOMID patients (18, 21). Somatic mosaicism for *NLRP3* mutations is observed in some sporadic cases of NOMID, as well as the closely related autoinflammatory disorder Schnitzler syndrome (22), but is rarely associated with the other milder phenotypes (23, 24).

Audiologic and radiologic studies of NOMID or MWS patients reveal that *NLRP3* mutations cause hearing loss by affecting cochlear function. Pathologic enhancement is observed on postcontrast MRI of the cochlea with fluid-attenuation inversion recovery (MRI-FLAIR). This finding indicates an increase in blood flow, vascular permeability, or both, and suggests the presence of cochlear inflammation (11, 16). The cochlea could be a peripheral secondary target of systemic autoinflammation, but it is also plausible that autoinflammation is a local process originating within the inner ear. Recent studies have demonstrated that the mouse cochlea harbors cells that are immunoreactive with immune cell-specific markers under normal resting conditions (25–27), as well as in pathogenic disorders of hearing. In an *Slc26a4*-insufficient mouse model of hearing loss in human DFNB4 nonsyndromic deafness and Pendred syndrome, hearing loss is associated with an increase in staining of macrophage/monocyte-like cells in the cochlea (28). It is unknown if these cells mediate local innate immune responses through activation of the NLRP3 inflammasome within the cochlea. Since *SLC26A4* mutations are one of the two most common causes of genetic hearing loss worldwide, innate immune mechanisms within the cochlea may be relevant to a wide variety of hearing-loss disorders.

Inner ear tissues and cells cannot be accessed in living humans without major surgery and a high risk of permanent deafness and dizziness. Therefore, mouse models are essential to understand the pathogenesis of molecular-genetic disorders of hearing loss. *Nlrp3* knockin mouse models of CAPS have been generated (29–31) but exhibit growth delay, low body weight, and die before 2–3 wk of age. Since this is the age at which wild-type cochleae finally acquire normal auditory structure and function (32), mouse models have not yet provided insight into the pathogenesis of hearing loss caused by *NLRP3* mutations.

In this study, we show that a missense mutation in the LRR domain of *NLRP3* can cause hearing loss as a prominent feature of an atypical CAPS phenotype or as a nonsyndromic phenotype with no other signs or symptoms. Anakinra treatment reversed or reduced the level of hearing loss in some patients. We demonstrate that resident cells in the mouse cochlea express *Nlrp3* and can secrete IL-1β, and could thus mediate local autoinflammation through activation of the NLRP3 inflammasome. This pathway might underlie other hearing-loss disorders that could be treated with IL-1β blockade therapy.

Results

Family LMG113 Segregates Nonsyndromic Hearing Loss. Three generations of a North American Caucasian family, LMG113, segregated sensorineural hearing loss (audiograms at initial ascertainment shown in Fig. 1). Multiple cases of male-to-male transmission and similar phenotypic severity between affected males and affected females were consistent with autosomal dominant inheritance. Their hearing loss was bilateral, symmetric, and progressive. The age of onset was self-reported to vary from the late second to fourth decade of life. We were unable to detect any cosegregating phenotypic features. Subject 1285 had progressive neuromuscular weakness, beginning at 45 y of age, which was eventually diagnosed as multiple sclerosis (MS) at an outside health care facility. Subject 1189 had episodic edema of her lower extremities at the age of 43 y and was thought to have connective tissue disease but did not meet the criteria for any definitive diagnosis. Subject 1236 had a remote history of self-limited arthritis of unknown etiology in her third decade of life. None of these subjects or other family members had physical signs or symptoms meeting diagnostic criteria for CAPS.

DFNA34 Maps to Chromosome 1q44. A genome-wide linkage scan of hearing loss in family LMG113 yielded a maximum two-point logarithm of odds (LOD) (5) score of 3.15 with short tandem repeat (STR) markers on chromosome 1q44. We designated this locus as DFNA34 (33). The nomenclature for phenotypes and loci associated with autosomal dominant inheritance is "DFNA," followed by an Arabic numeral denoting the order in which the locus was discovered. We also performed a genome-wide linkage analysis with SNP markers that revealed a positive region (maximum LOD = 2.94) between markers rs974893 and rs2027432 on chromosome 1q43-1q44 (Fig. 2A). We also identified other loci with LOD scores > 1.5 on chromosomes 4, 7, 11, 16, and 17. However, these loci were all excluded on the basis of discordant segregation of hearing loss with combined STR-SNP haplotypes. Fine-mapping with novel microsatellite markers on chromosome 1 narrowed the critical interval to 3.93 Mb with
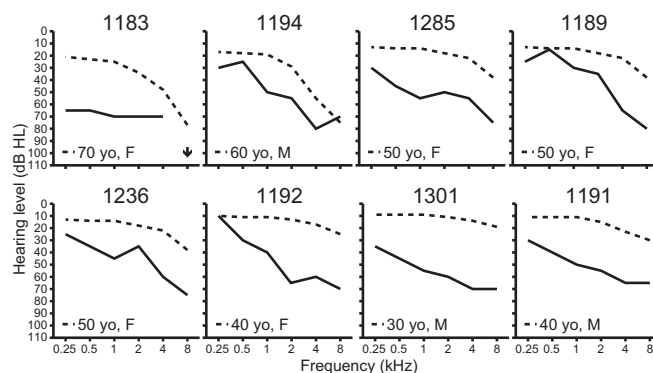
Fig. 1. Auditory phenotypes. Air-conduction hearing thresholds in the better-hearing ear of affected LMG113 family members at initial ascertainment. Subject identification numbers are shown at the top of each panel. Dashed lines denote the 90th-percentile of gender- and age-matched air-conduction normative thresholds from the International Organization for Standardization ISO 7029 (52). An arrow indicates that no response was obtained at the tested frequency.

a maximum LOD score of 3.51 between markers D1S102 and D1NIH10 (Fig. 2*B*).

DFNA34 Caused by *NLRP3* Mutation. The DFNA34 interval includes 36 RefSeq-annotated protein-coding genes, one of which is *NLRP3*. Dideoxy sequence analysis of *NLRP3* identified a heterozygous transition c.2753G > A (NM_001243133.1) in exon 7, predicted to result in the missense substitution p.Arg918Gln in the LRR domain of NLRP3 (NP_001230062.1) (Fig. 2 *C* and *D*). The arginine residue at position 918 is conserved in mammalian (chimpanzee, monkey, rat, mouse, dog, and rabbit) orthologous genes, but is not conserved in birds (chicken). Nucleotide sequence analysis of the rest of the participating members of family LMG113 confirmed that p.Arg918Gln cosegregated with hearing loss. We also completed dideoxy nucleotide sequence analysis and failed to detect c.2753G > A among 572 chromosomes from 286 North American ethnically matched control subjects. Finally, c.2753G > A was not present among ≈120,000 chromosomes on the Exome Aggregation Consortium (ExAC) browser (exac.broadinstitute.org; accessed January 19, 2017).

To exclude the possibility that variants in other genes cause hearing loss in family LMG113, we performed dideoxy sequence analysis of all coding and noncoding annotated exons of the other genes in the DFNA34 interval of genomic DNA from subject 1301. Seventy-three of 74 detected variants were annotated in dbSNP with allele frequencies > 0.01 (https://www.ncbi.nlm.nih.gov/projects/SNP; accessed January 19, 2017), leading us to conclude they were not pathogenic. One variant, c.371_391del

Fig. 2. Mutation analysis. (*A*) Genome-wide linkage analysis with SNP markers defined a peak with a maximum LOD score of 2.94 (arrow) on chromosome 1q43-1q44 between markers rs974893 and rs2027432. (*B*) Fine mapping with novel microsatellite markers narrowed the DFNA34 interval to 3.93 Mb with a maximum LOD score of 3.51 between markers D1S102 and D1NIH10. Coordinates are based on the GRCh38 human reference sequence. (*C*) Sequence chromatogram showing the heterozygous transition c.2753G > A (p.Arg918Gln) of *NLRP3* found in affected individuals. Nucleotide numbering is based on cDNA sequence (GenBank accession no. NM_001243133.1). (*D*) Arginine-918 is located in the LRR domain of NLRP3.

(NM_001001959.1) in *OR11L1*, is not annotated in the dbSNP or the ExAC browser (accessed January 19, 2017), but does not cosegregate with hearing loss in family LMG113. These results suggested that the p.Arg918Gln missense substitution of *NLRP3* was the pathogenic mutation causing DFNA34 hearing loss in family LMG113.

Reascertainment of LMG113 for CAPS. Due to the causal association of other *NLRP3* mutations with CAPS, we reascertained LMG113 family members 1189, 1236, and 1238 at the NIH Clinical Center. Subject 1236 was then a 59-y-old female with bilateral, symmetric, progressive sensorineural hearing loss since her fourth decade of life (Fig. 1). She reported a history of arthritis affecting both hands and one knee in her third decade of life. The symptoms and signs resolved and did not recur. An etiology or diagnosis was never established. She denied any subsequent arthritic signs or symptoms. She did not have any mucocutaneous signs or symptoms of the nasal or oral cavities or skin. She denied gastrointestinal symptoms and had no history of fever, myalgia, arthralgia, cold sensitivity, or other medical conditions. She had no abnormal findings on physical examination by a rheumatologist.

Subject 1236 had elevated serologic markers of inflammation: C-reactive protein (CRP) = 7.96 mg/L, fibrinogen = 509 mg/dL, and erythrocyte sedimentation rate (ESR) = 38 mm/h (Fig. 3*A*). Her cultured peripheral-blood mononuclear cells (PBMCs) secreted high levels of IL-1β in response to stimulation with LPS, compared with nondetectable levels of IL-1β secreted by healthy control PBMCs (Fig. 3*B*). This showed that p.Arg918Gln is a gain-of-function mutation that results in an elevated baseline state for IL-1β secretion. Postcontrast MRI-FLAIR examination of the temporal bones of subject 1236 revealed pathologic enhancement of the cochlea (Fig. 3*C*) that was similar to—but less severe than—what is typically observed in NOMID or MWS patients with sensorineural hearing loss.

We concluded that subject 1236 had hearing loss and autoinflammation due to the p.Arg918Gln mutation of *NLRP3*. After 3 mo of subcutaneous anakinra administration (100 mg/d), her serologic markers of inflammation normalized to CRP = 0.6 mg/L, fibrinogen = 298 mg/dL, and ESR = 8 mm/h (Fig. 3*A*). Her hearing did not subjectively change. Her mean hearing thresholds (0.5/1/2/4-kHz) were 64 dB HL in each ear immediately before anakinra treatment. Her mean hearing threshold was 63 dB HL in the right ear and 59 dB HL in the left ear after 110 d of anakinra (Fig. 3*D*). Postanakinra MRI-FLAIR was also performed but could not be interpreted due to technical reasons.

Subject 1189 was a 63-y-old female with bilateral, symmetric, progressive sensorineural hearing loss (Fig. 1). She reported a history of idiopathic edema in her lower extremities at 43 y of age. The symptoms and signs resolved and did not recur. She had no mucocutaneous signs or symptoms of the nasal or oral cavities or skin. She denied gastrointestinal symptoms and had no history of fever, myalgia, arthralgia, cold sensitivity, or other medical conditions. She had no abnormal findings on physical examination by a rheumatologist. Her ESR was slightly elevated (56.0 mm/h) but her CRP and fibrinogen levels were within normal limits (Table S1). Her cultured PBMCs secreted abnormal high levels of IL-1β in response to stimulation with LPS (Fig. S2*A*). Postcontrast MRI-FLAIR examination of the temporal bones revealed pathologic enhancement of the cochlea (Table S1). Subjects 1189 and 1236, therefore, both had sensorineural hearing loss associated with radiologic evidence of cochlear inflammation.

We also evaluated subject 1238, the 32-y-old daughter of subject 1236, who carried the p.Arg918Gln mutation of *NLRP3*. Her pure-tone audiometric thresholds were normal (<20 dB HL) and the results of a postcontrast MRI-FLAIR study of her temporal bones showed no evidence of enhancement (Table S1). Her medical history was remarkable for idiopathic subglottic stenosis at the age of 25 y old, requiring a tracheotomy and
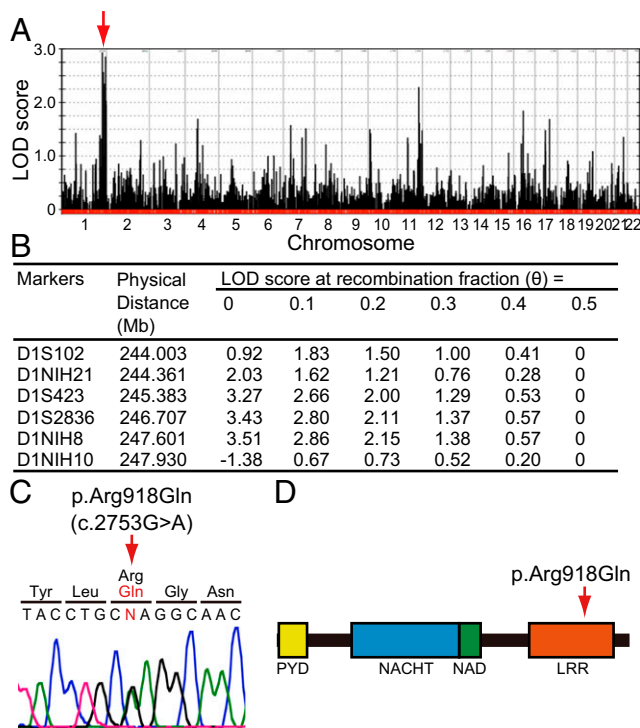
A

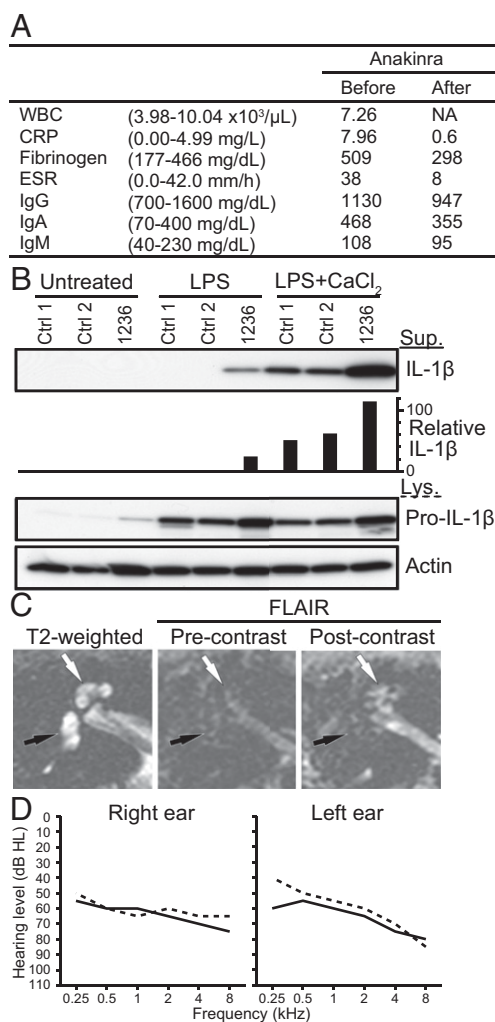|		Anakinra	
		Before	After
WBC	(3.98-10.04 x10³/μL)	7.26	NA
CRP	(0.00-4.99 mg/L)	7.96	0.6
Fibrinogen	(177-466 mg/dL)	509	298
ESR	(0.0-42.0 mm/h)	38	8
IgG	(700-1600 mg/dL)	1130	947
IgA	(70-400 mg/dL)	468	355
IgM	(40-230 mg/dL)	108	95

Fig. 3. Phenotype of subject 1236. (A) Serological test results before and after anakinra administration. The normal range is shown in parentheses. WBC data after the administration was not available (NA). WBC, CRP, ESR, and IgG indicate white blood cell count, C-reactive protein, erythrocyte sedimentation rate, and IgG, respectively. (B) IL-1β was secreted from the patient's cultured PBMCs in response to LPS, compared with nondetectable levels secreted by normal control (Ctrl) cells. In response to LPS with CaCl₂, an increased level of IL-1β was secreted from the patient's PBMCs compared with those from control PBMCs. IL-1β was measured in the supernatant (Sup.), whereas pro–IL-1β and actin was measured in the cell lysate (Lys.). Relative IL-1β levels were determined by densitometry analysis of released IL-1β in supernatants, normalized to actin. (C) Magnetic resonance images of the right temporal bone of subject 1236 before anakinra administration. Axial T2-weighted image (Left) shows the normal high signal from fluid throughout the cochlea (white arrow) and vestibule (black arrow). Axial imaging with MRI-FLAIR (Center) without contrast demonstrates the normally suppressed fluid signal from both cochlea and vestibule (arrows). An axial FLAIR image obtained after intravenous contrast (Right) demonstrates high signal in the cochlea (white arrow) but not the vestibule (black arrow), indicating accumulation of contrast from inflammatory changes. (D) Pure-tone air-conduction thresholds before (solid lines) and after (dashed lines) anakinra administration.

multiple surgical dilations with local corticosteroid injections until the age of 28 y. The stenosis resolved to a level permitting tracheostomy decannulation and no further treatment. She had no specific signs or symptoms of systemic inflammation. Her serologic tests of inflammation were within normal limits (Table S1) but her PBMCs secreted abnormal high levels of IL-1β in response to stimulation with LPS (Fig. S2A).

NLRP3 Mutation Causes Syndromic Hearing Loss in Family LMG446.
We subsequently ascertained the affected members of LMG446, an unrelated North American family of mixed Caucasian and Hispanic ancestry, segregating sensorineural hearing loss, mixed signs and symptoms of systemic autoinflammation, and the c.2753G > A (p.Arg918Gln) mutation of NLRP3 (Fig. 4A). The father, subject 2261, was 35 y old with a history of progressive bilateral sensorineural hearing loss (Fig. 5), episodic urticaria that could be precipitated by pressure (Fig. 4C), and periodic fevers, conjunctivitis, oral ulcers, and cervical lymphadenopathy (Table S2). He also reported left knee arthritis, multiarticular arthralgia, left shoulder bursitis, and migraine headaches (Table S2). His three offspring (subjects 2262, 2264, and 2265) all carried the p.Arg918Gln mutation and were reported to have periodic fevers, conjunctivitis, oral ulcers, cervical lymphadenopathy, and headaches. Subject 2262 (13 y old) had bilateral hearing loss at 6 and 8 kHz, subject 2264 (10 y old) had right-sided hearing loss at 6 and 8 kHz, and subject 2265 (6 y old) had hearing thresholds within normal limits (Fig. 5). Subjects 2262 and 2264 also had episodic urticaria (Fig. 4C). MRI-FLAIR evaluations of their temporal bones demonstrated abnormally increased signal, before the administration of contrast, in both ears of subjects 2261 (Fig. 4B), 2262, and 2265, and the right ear of subject 2264 (Table S2). This reflects elevated protein concentration in perilymph and is probable evidence of prior inflammation. There was postcontrast enhancement of the cochleae in both ears of subjects 2261 (Fig. 4B) and 2262 but not in subjects 2264 or 2265 (Table S2). The ESR, CRP, and fibrinogen levels were all within normal limits in affected members of LMG446 (Table S2). However, PBMCs from subjects 2262, 2264, and 2265 all showed abnormal high secretion of IL-1β in response to stimulation with LPS (Fig. S2 B–D) (cells from subject 2261 were not tested). These data for family LMG446 broaden the phenotypic spectrum of the p.Arg918Gln mutation of NLRP3 beyond nonsyndromic hearing loss to a novel form of CAPS.

Founder Effect for the NLRP3 Mutation in Families LMG113 and LMG446. We performed a comparative genotype-haplotype analysis of SNP and STR markers closely linked to the p.Arg918Gln mutation segregating in LMG113 and LMG446. We identified three informative SNPs (rs3806268, rs4925543, and rs34298354) within exon 3 of NLRP3, with shared alleles (A/G/T) between the mutant chromosomes in the two families. This three-SNP haplotype is present in 22 (11.1%) of 198 Caucasian Europeans in the 1000 Genomes database (www.internationalgenome.org; accessed June 3, 2016). These results suggest that the p.Arg918Gln mutation in LMG113 and LMG446 could have arisen from a common founder.

IL-1β Blockade Reverses Hearing Loss in Family LMG446. Subjects 2261, 2262, and 2264 were treated with subcutaneous anakinra at 200 mg (2261) or 100 mg (2262, 2264) daily. After 5 mo of therapy, the pure-tone audiometric thresholds of the children (2262, 2264) were completely within normal limits (≤15 dB HL) (Fig. 5). The thresholds of subject 2261 (father) improved to within 90th-percentile age- and gender-matched normative thresholds for the left ear (except for 5 dB below the norm in response to the 0.25-kHz stimulus), whereas the right ear showed no significant (>10 dB) improvement at any stimulus frequency (Fig. 5). The improvements in hearing correlated with a decrease in precontrast MRI-FLAIR signal in the right ear of subject 2264, as well as decreases in postcontrast enhancement in the left ear of subject 2261 and both ears of subject 2262. Other signs and symptoms of autoinflammation were reportedly improved or resolved.

NLRP3 Inflammasome Pathway Gene Expression in Mouse Cochlea. We hypothesized that cochlear inflammation can be induced through one or both of two mechanisms. First, the cochlea could be a secondary target organ of systemic autoinflammation mediated
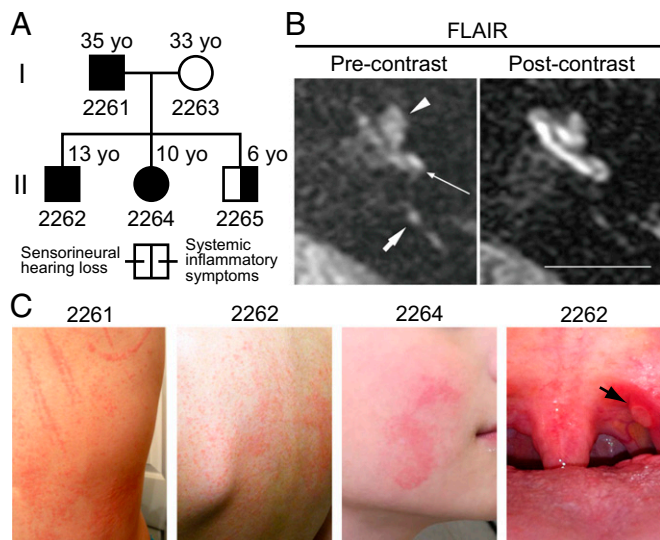
Fig. 4. Family LMG446 phenotype. (*A*) Family LMG446 pedigree showing segregation of the p.Arg918Gln mutation of *NLRP3* with hearing loss and signs and symptoms of systemic autoinflammation. (*B*) MRI of subject 2261 using FLAIR before contrast administration demonstrates increased signal of perilymph due to elevated protein concentration in the basal (long thin arrow) and apical (arrowhead) turns of the cochlea, suggestive of prior inflammation (*Left*). Short arrow indicates the posterior semicircular canal. There was enhanced postcontrast signal in the basal and apical turns of the cochlea representing accumulation of contrast from inflammation (*Right*). (Scale bar, 1 cm.) (*C*) Urticaria shown on subjects 2261 and 2262 and on the right cheek of subject 2264. An oral ulcer (black arrow) is shown on the left tonsillar pillar of subject 2262.

by the activation of the NLRP3 inflammasome and secretion of IL-1β by circulating immune cells. Alternatively, the NLRP3 inflammasome could be activated within resident cells of the cochlea to secrete IL-1β. We tested this latter hypothesis by evaluating expression of *Nlrp3* and other genes in the NLRP3 inflammasome activation pathway in wild-type mouse cochleae. RT-PCR analysis detected *Nlrp3*, *Pycard* (encoding ASC), *Casp1*, and *Il1b* mRNA in adult wild-type mouse cochleae (Fig. 6*A*). The RNA levels for each gene were all within a fivefold range of the corresponding levels in other tissues (brain, lung, and liver) in which the NLRP3 inflammasome has been reported to exist (34–36) (Fig. 6*B*). This variance could be due to differing proportions of NLRP3+ cells among these tissues. Quantitative RT-PCR analysis of mouse cochlear RNA at different time points revealed that the levels of *Nlrp3*, *Pycard*, and *Casp1* mRNA increased by two- to threefold at postnatal day 4 (P4) and P8 compared with those at P0, and remained constant at P28 (Fig. 6*C*). The *Il1b* mRNA level increased by 10- to 12-fold at P8 and P28 compared with the levels at P0 and P4. These results indicate that unstimulated wild-type mouse cochleae express mRNAs encoding key proteins required for activation of the NLRP3 inflammasome and secretion of IL-1β.

Tissue-Resident Macrophage-Like Cells in Mouse Cochlea. The NLRP3 inflammasome is typically present in innate immune cells, including monocytes, macrophages, and dendritic cells (2–4). We examined if innate immune-lineage cells exist in the cochlea using *Cx3cr1*^GFP mice in which the *Cx3cr1* gene is replaced with cDNA encoding GFP. *Cx3cr1* encodes Cx3cr1, a chemokine receptor expressed in mouse monocytes, as well as in subsets of NK cells, dendritic cells, and resident macrophages (37). After P0, we detected GFP+ cells scattered throughout all *Cx3cr1*^GFP/+ cochlear tissues, including the auditory nerve, spiral ganglion, basilar membrane, stria vascularis, and spiral ligament (Fig. 7*A* and Fig. S3). In the lateral wall and basilar membrane, the GFP+ cells were

primarily located adjacent to or near blood vessels (Fig. 7*B* and Figs. S4 and S5). Anti-F4/80 antibodies also bound the GFP+ cells (Fig. 7*C* and Fig. S6). F4/80 is a marker of mature macrophages (38, 39), indicating that the GFP+ cells in *Cx3cr1*^GFP cochleae represent tissue-resident macrophage-like cells.

Cochlea-Resident Macrophage-Like Cells Express *Nlrp3*. We sought to determine if *Nlrp3* is expressed in cochlea-resident cells expressing *Cx3cr1*, a nonspecific marker for monocytes and lymphocytes. We used FACS to isolate GFP+ cells from 19-d old *Cx3cr1*^GFP mouse cochleae. RT-PCR analysis detected *Nlrp3* mRNA in GFP+ cells but not in GFP− cells from the same FACS procedure (Fig. 8). We did not attempt to detect NLRP3 protein due to a lack of specific antibodies. mRNA encoding CD45, also known as leukocyte-common antigen, was detected in both GFP+ and GFP− cochlear cell populations, whereas only GFP+ cells expressed the murine macrophage marker F4/80. These results indicate that, although other leukocytes may be present, only the macrophage-like cells in the normal mouse cochlea express *Nlrp3*.

NLRP3 Inflammasome Activity in Mouse Cochlea. To examine if the NLRP3 inflammasome can be activated in wild-type cochleae, we measured IL-1β levels in supernatants of P3–P4 wild-type mouse cochlear tissues grown in culture under one of three conditions according to a standard protocol (31): no stimulation, stimulation with LPS, or stimulation with LPS pulsed with ATP (designated LPS+ATP). Significantly higher levels of IL-1β were secreted from cultured cochleae stimulated with LPS+ATP, compared with those in the absence of ATP (*P* < 0.01) (Fig. 9*A*). Quantitative RT-PCR analysis of the cultured tissues revealed that *Il1b* mRNA levels were significantly increased even in the absence of ATP (*P* < 0.001) (Fig. 9*B*), indicating that costimulation with ATP was critical for IL-1β secretion. IL-1β was not secreted from cultured *Nlrp3*^Δ/Δ cochleae stimulated with LPS+ATP (Fig. 9*C*), although *Il1b* mRNA levels were significantly increased (Fig. 9*D*). These results indicate that IL-1β release induced by stimulation with LPS pulsed with ATP predominantly results from NLRP3 inflammasome activation (40).
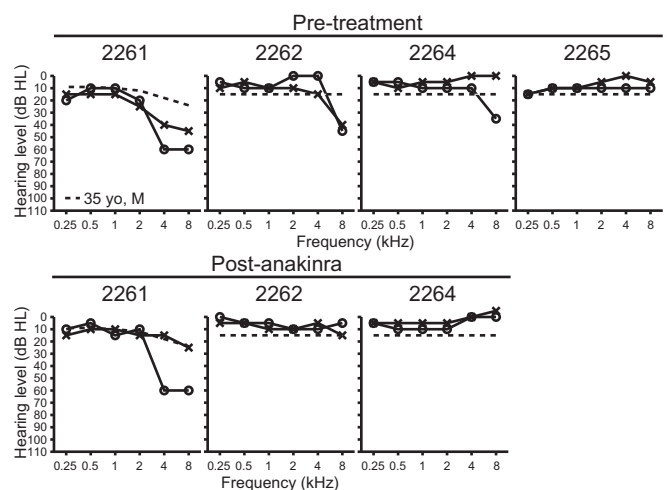

Fig. 5. Family LMG446 auditory phenotype. Pure-tone air-conduction thresholds in affected members of family LMG446 before (*Upper*) and after (*Lower*) 5 mo of treatment with anakinra. O, right ear thresholds; X, left ear thresholds. Dashed line for subject 2261 denotes the 90th-percentile of gender- and age-matched air-conduction normative thresholds from the International Organization for Standardization ISO 7029 (52). Dashed lines at 15 dB HL for subjects 2262, 2264, and 2265 indicate normal threshold limits for pediatric populations.
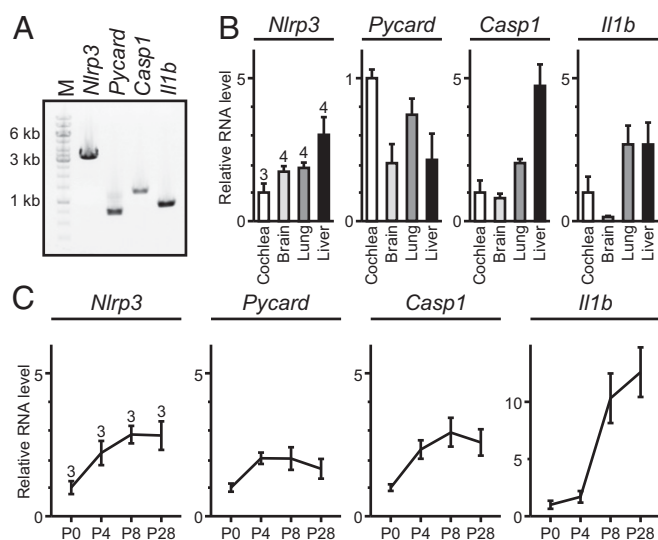
Fig. 6. *Nlrp3, Pycard, Casp1,* and *Il1b* expression in mouse cochlea. (*A*) RT-PCR analysis of *Nlrp3, Pycard, Casp1,* and *Il1b* mRNA expression in adult wild-type mouse cochlea harvested at P30. PCR primers were designed to amplify *Nlrp3* (3,312 bp), *Pycard* (752 bp), *Casp1* (1,352 bp), or *Il1b* (908 bp) cDNA including all of the coding sequences. PCR amplification included 35 cycles. "M" indicates the 1-kb molecular marker ladder. (*B*) Quantitative RT-PCR analysis showed that *Nlrp3, Pycard, Casp1,* and *Il1b* mRNA levels (mean ± SD) in the adult mouse cochlea (P30) were within an order-of-magnitude of those in other tissues including brain, lung, and liver. For each bar the upper number indicates the number of mice examined. The mRNA level in other tissues was first normalized to the *Actb* level and then to the level in the cochlea. (*C*) Quantitative RT-PCR analysis of mouse cochlear RNA shows developmental changes in *Nlrp3, Pycard, Casp1,* and *Il1b* mRNA levels (mean ± SD). For each bar the upper number indicates the number of mice examined. The mRNA level for each gene was first normalized to the *Actb* level and then to its own value measured at P0.

We then measured the IL-1β concentrations in supernatants of cultures of portions (organ of Corti, lateral wall, or auditory nerve) of the cochleae that had been microdissected and cultured separately (illustrated in Fig. S3). Higher levels of IL-1β were secreted from each portion of the cochlea in response to LPS+ATP, with the maximum released from auditory nerve tissue, compared with levels of IL-1β secreted in the absence of ATP (Fig. 10*A*). This finding indicates that the NLRP3 inflammasome exists and can be activated in cells in all of these regions of the cochlea.

To identify the cochlear cells in which the NLRP3 inflammasome was activated, we used anti–IL-1β antibodies to stain cultured P4 *Cx3cr1*[GFP/+] cochleae after LPS stimulation. IL-1β immunoreactivity was detected only in a subset of GFP+ cells from the stimulated tissues, while no immunoreactivity was detected in the absence of stimulation (Fig. 10*B* and Fig. S7). This observation indicates that IL-1β expression was elevated in some Cx3cr1+ cells in response to LPS stimulation. We conclude that these macrophage/monocyte-like cells are the cochlear cells in which the NLRP3 inflammasome exists and can be activated.

Discussion

Mutation in *NLRP3* Causes DFNA34. Here we show that a missense amino acid substitution of the *NLRP3* gene causes DFNA34 hearing loss in family LMG113. Our initial ascertainment suggested the hearing loss was nonsyndromic, although a few affected subjects had clinical features in addition to hearing loss. Subject 1285 was diagnosed with MS at 45 y of age, and there are two reports of MS-like lesions in CAPS patients (41, 42). Furthermore, experimental autoimmune encephalomyelitis developed more slowly and was less severe in *Nlrp3*^{−/−} mice than in wild-type mice, thus implicating *Nlrp3*

in disease progression in an animal model of MS (43). The MS-like disease in subject 1285 may therefore somehow be related to her *NLRP3* mutation. Subjects 1189 and 1236 had nonspecific signs and symptoms that could have been related to autoinflammation but were neither diagnostic of CAPS nor other discrete clinical entities. The relationship of these other clinical features to their *NLRP3* mutation thus remains unknown. Physical examination of subject 1236 at the time of reascertainment revealed no evidence of CAPS. However, serological testing revealed asymptomatic low-grade systemic inflammation. Furthermore, the PBMCs from all three tested members of LMG113 showed the pathologic secretion of IL-1β that characteristically reflects gain-of-function mutations of *NLRP3* in CAPS. There was no evidence of physical signs or symptoms of CAPS in the remainder of the family.

In contrast, LMG446 segregated the same mutation of *NLRP3* with hearing loss and other clinical features as part of a syndrome. Their systemic autoinflammatory phenotype is atypical for CAPS since none of them met diagnostic criteria for MWS, NOMID, or FCAS. The auditory phenotype in LMG446 was also different from that segregating in LMG113. The onset was during the first decade of life in all of the LMG446 mutation carriers except subject 2265, whose normal hearing may reflect his young age and, thus, presymptomatic status. This is in contrast to LMG113 in which the hearing loss does not manifest until the late second to fourth decade of life. It is not unprecedented for an *NLRP3* mutation to be associated with different phenotypes in different families or even different individuals, possibly due to the influence of genetic or environmental modifiers. However, one commonality among the phenotypes segregating in the two families is that hearing loss is the most prominent objective finding associated with the p.Arg918Gln mutation.

Genetic studies of patients with CAPS have identified more than 80 disease-associated variants in *NLRP3*. Most of the variants are missense substitutions affecting the NACHT domain, encoded by exon 3 (19). In contrast, the DFNA34 mutation affects the LRR domain. Mutations in the LRR domain are associated with atypical or milder phenotypes (19). Although the
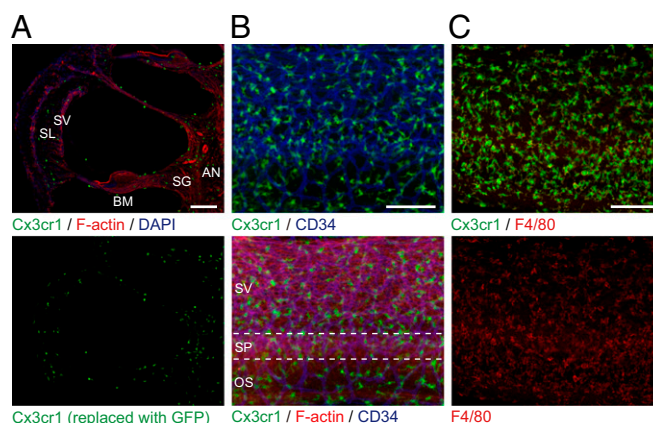

Fig. 7. Distribution of resident macrophage-like cells in mouse cochlea. (*A*) Frozen sections of P4 *Cx3cr1*[GFP/+] cochlea show GFP+ cells distributed in all parts of the cochlea, including the auditory nerve (AN), spiral ganglion (SG), basilar membrane (BM), stria vascularis (SV), and spiral ligament (SL). Sections were counterstained with phalloidin (red) and DAPI (blue) to identify F-actin and nuclei, respectively. (*B*) Whole-mount preparation of lateral wall of P4 *Cx3cr1*[GFP/+] cochlea stained with CD34 antibody (blue) shows GFP+ cells are mainly located around blood vessels. Anti-CD34 antibody specifically stains vascular endothelium in the inner ear (59). Tissues were counterstained with phalloidin (red). SV, SP, and OS indicate stria vascularis, spiral prominence, and outer sulcus, respectively. (*C*) Whole-mount preparation of lateral wall of P4 *Cx3cr1*[GFP/+] cochlea stained with F4/80 antibody (red) shows that GFP+ cells are costained with F4/80, indicating these cells have macrophage characteristics. (Scale bars, 100 μm.)
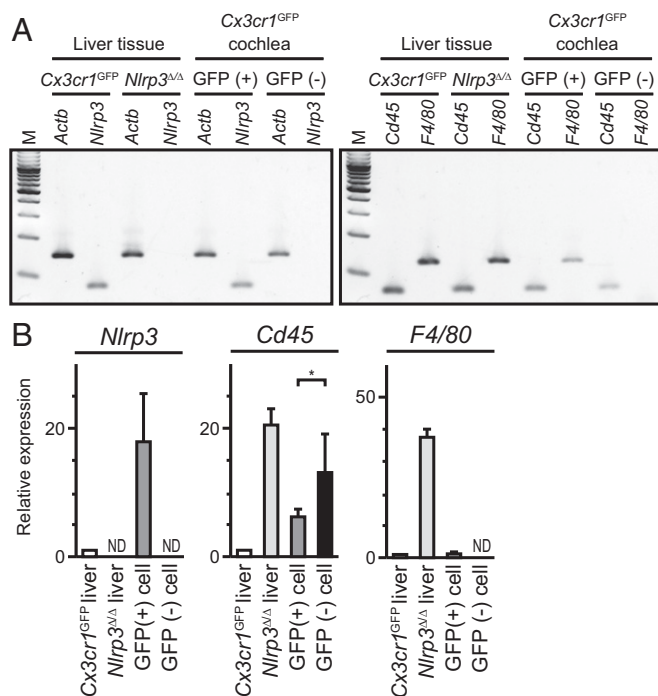
Fig. 8. *Nlrp3* expression in resident macrophage-like cells of mouse cochlea. (*A*) Agarose gel electrophoresis of RT-PCR products demonstrating the existence of *Nlrp3* (*Left*) and *Cd45* (WBC marker, *Right*) and *F4/80* (murine macrophage marker, *Right*) mRNA expression within the normal mouse cochlea. *Cx3cr1^{GFP}* cochlear cells were separated by FACS to isolate GFP$^+$ and GFP$^-$ cell populations for RNA purification and RT-PCR analysis. (*B*) Quantitative RT-PCR analysis demonstrated differential expression of *Nlrp3*, *Cd45*, *F4/80* mRNA (mean ± SD) in GFP$^+$ and GFP$^-$ cells from P19 *Cx3cr1^{GFP}* mouse cochleae. The observed difference in *Cd45* mRNA levels between GFP$^+$ and GFP$^-$ cells was significant (unpaired *t* test, *$P < 0.05$). *Nlrp3* and *F4/80* mRNA were not detected (ND) in GFP$^-$ cells. The mRNA level in each sample was first normalized to the *Actb* level and then to the level in the liver of *Cx3cr1^{GFP}* mice. Liver samples from *Cx3cr1^{GFP}* mice and *Nlrp3$^{Δ/Δ}$* mice served as positive and negative controls for *Nlrp3* expression.

LRRs are believed to maintain NLRP3 in an autosuppressed state (7), the molecular mechanism of mutations leading to atypical phenotypes remains unknown.

IL-1β Receptor Blockade Therapy for Hearing Loss. Anakinra administration did not noticeably affect hearing loss in subject 1236 (Fig. 3*D*), although the treatment and observation periods were brief in comparison with the long, gradual rate of her acquisition of hearing loss. However, anakinra therapy reversed the hearing loss in subjects 2262 and 2264, and improved the hearing loss in one ear of subject 2261 (Fig. 5). Some studies have indeed reported efficacy of anakinra for stabilizing or reversing hearing loss in a subset of CAPS patients treated with anakinra (18, 21, 44). Our observations are consistent with the concept of a therapeutic window of opportunity preceding or occurring soon after the onset of hearing loss since it appears to be irreversible at later ages (18, 44). Hearing loss in our 59-y-old subject 1236 might have been irreversible due to its long duration, but we cannot exclude the possibility that anakinra treatment was insufficient in duration or dosage. It is unknown if anakinra acts locally within cochlear tissues to prevent or reverse hearing loss. Therefore, the dosage regimens for systemic anakinra administration that are adequate in other sites of disease manifestations may not produce equally therapeutic levels within the cochlea.

Pathogenesis of DFNA34. The pathologic enhancement of the cochlea in MRI-FLAIR studies (Figs. 3*C* and 4*B*) of our subjects,

or NOMID or MWS patients with hearing loss (11, 16), strongly implicates cochlear inflammation in the pathogenesis of hearing loss. This raises the important question of whether this is a result of systemic inflammation with cochlear infiltration of circulating immune cells, pathologic activation of the NLRP3 inflammasome within resident immune cells of the cochlea, or a combination of these mechanisms. The different phenotypes segregating in families LMG113 and LMG446 may indeed reflect different or multiple immune-mediated mechanisms for hearing loss. It is possible that the magnitude of cochlear inflammation parallels systemic symptoms, and thus the pauci-symptomatic cases reported here manifest a relatively late onset of hearing loss.

During normal development, there are initial populations of tissue-resident macrophages that are thought to derive from the yolk sac (45). Subsequently, macrophage precursors arise from the hematopoietic stem cell lineage and enter the circulation as monocytes that differentiate into macrophages or dendritic cells when they migrate into tissues. Macrophages reside in tissues as tissue-resident macrophages in steady state, and are also recruited into tissues as infiltrating macrophages in response to inflammation (46). The existence of macrophage-like cells in adult mouse cochlea has been demonstrated in previous reports. Hirose et al. (25) reported GFP$^+$ cells in adult *Cx3cr1$^{GFP/GFP}$* mouse cochlea, which expressed a lymphocyte marker CD45 and macrophage markers
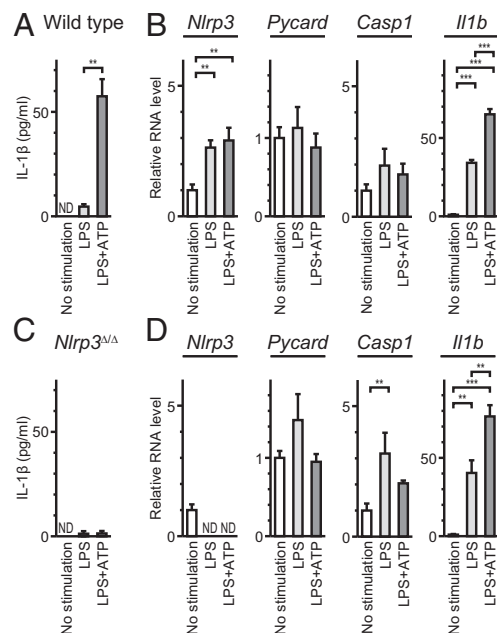

Fig. 9. Activation of NLRP3 inflammasome in mouse cochlea. (*A*) IL-1β levels (mean ± SD) in culture supernatant (total volume = 1.0 mL) from eight wild-type cochleae. Significantly larger amounts of IL-1β were secreted from cultured cochleae in response to LPS+ATP, compared with that in the absence of ATP (unpaired *t* test, *$P < 0.01$). IL-1β was not detected (ND) in supernatant from cultured cochlea without stimulation. (*B*) Quantitative RT-PCR analysis of cultured wild-type cochleae. *Nlrp3* and *Il1b* mRNA levels (mean ± SD) were significantly different among each group (one-way ANOVA, **$P < 0.01$ or ***$P < 0.001$, respectively). *Nlrp3* and *Il1b* mRNA levels increased in response to LPS compared with levels in the absence of stimulation (Tukey post hoc test: $P < 0.01$, $P < 0.001$, respectively). mRNA levels were normalized first to the *Actb* level and then to the expression level without stimulation. (*C*) IL-1β levels secreted from cultured *Nlrp3$^{Δ/Δ}$* cochleae in response to LPS+ATP were not significantly different from those in the absence of ATP. (*D*) In *Nlrp3$^{Δ/Δ}$* cochleae, *Casp1* and *Il1b* mRNA levels were significantly different (one-way ANOVA, $P < 0.01$ or $P < 0.001$, respectively). *Casp1* and *Il1b* mRNA levels increased in response to LPS compared with levels in the absence of stimulation (Tukey post hoc test: $P < 0.001$, $P < 0.001$, respectively). mRNA levels were normalized first to the *Actb* level and then to the expression level without stimulation of cultured wild-type cochleae.
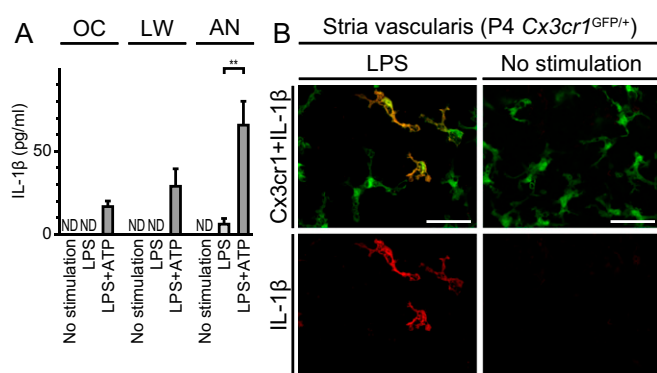
Fig. 10. Characteristics of NLRP3 inflammasome in mouse cochlea. (*A*) IL-1β levels (mean ± SD) measured in supernatants (total volume 0.4 mL) from three separately cultured parts of the cochleae: organ of Corti (OC), lateral wall (LW), or auditory nerve (AN). Higher levels of IL-1β were secreted from each part of the cochleae in response to LPS+ATP with the maximum released from the auditory nerve, compared with those in the absence of ATP stimulation (unpaired *t* test, **P < 0.01 for AN). (*B*) Whole-mount preparation of cultured lateral wall of P4 *Cx3cr1*^GFP/+ cochlea stained with anti-IL-1β antibody (red). IL-1β immunoreactivity was detected in a subset of GFP+ cells from cultured cochlea stimulated with LPS, whereas no immunoreactivity was detected in the absence of stimulation. (Scale bar, 50 μm.)

CD68 and Iba1. These GFP+ cells were likely to have been derived from bone marrow (47). Here, we showed that GFP+ cells were distributed in all parts of the cochlea, at least after P0, and located around blood vessels (Fig. 7 and Figs. S3–S5). They express another macrophage marker F4/80 (Fig. 7 and Figs. S4 and S6), supporting the conclusion that these GFP+ cells are tissue-resident macrophage/monocyte-like cells.

IL-1β secretion by bone marrow-derived macrophages stimulated with LPS+ATP is thought to require activation of the NLRP3 inflammasome (4, 40). Our findings thus indicate the existence of resident cells and molecules required for NLRP3 inflammasome activation in the cochlea. Our results are consistent with the hypothesis that locally secreted IL-1β within the cochlea can induce cochlear inflammation.

The role of IL-1β in hearing loss is supported by a recent study (48) in which anakinra improved hearing in 7 of 10 patients with corticosteroid-resistant "autoimmune inner ear disease." Plasma levels of IL-1β were associated with both clinical hearing response and disease relapse upon discontinuation of anakinra (48).

It was recently shown that ablation of *Nlrp3* expression in pancreatic islets, comprised of nonhematopoietic cells, can compromise migration of immune cells to pancreatic islets (49). This raises the possibility that nonhematopoietic cochlear cells can also express *NLRP3*/*Nlrp3* and contribute to cochlear autoinflammation in humans with DFNA34 or CAPS. However, our results suggest that Cx3cr1+;F4/80+ cells are the primary source of *Nlrp3* mRNA in mouse cochlea (Fig. 8). If nonhematopoietic cochlear cells do indeed express *Nlrp3*, it may be a phenomenon elicited by other factors, such as genetic or environmental modifiers. Differences in this pathway may also exist between humans and mice. Therefore, it remains possible that mutant NLRP3 expression in human nonhematopoietic cochlear cells can contribute to macrophage migration to the cochlea and cochlear autoinflammation in DFNA34 and CAPS.

In conclusion, we have shown that a mutation of the *NLRP3* gene can cause hearing loss in the absence of the other clinical signs and symptoms of CAPS that are associated with other mutations of *NLRP3*. We have shown that tissue-resident macrophage/monocyte-like cells in the mouse cochlea can be induced to express and activate the NLRP3 inflammasome. This suggests that activation of innate immune pathways within the cochlea may directly cause local cochlear autoinflammation. This mechanism may be a final common

pathway for hearing loss caused by a variety of factors that can activate innate immunity such as pathogens, chemicals, trauma, aging, or oxidative stress (50, 51). The existence of proven therapies to block the NLRP3 pathway and reverse or improve hearing loss merits future investigations of the role of NLRP3 within the cochlea and the pathogenesis of hearing loss associated with a wide variety of etiologies, both known and unknown.

Methods

Pedigree and Clinical Evaluations of Families LMG113 and LMG446. We initially ascertained the affected members of LMG113 at the NIH Clinical Center in 2000. We have not presented their pedigree to protect their privacy. The clinical evaluation consisted of a medical and developmental history interview and physical examination by an otolaryngologist head and neck surgeon. A rheumatologist also examined each family member with DFNA34 hearing loss. Audiological examination consisted of otoscopy, pure-tone audiometry (0.25–8 kHz), and tympanometry. Adult family members were designated as affected if they had an air-conduction threshold higher than the 90th-percentile of gender- and age-matched air-conduction thresholds for ≥3 tested stimulus frequencies (52). Pediatric subjects were considered to be affected if a threshold exceeded 15 dB HL (53).

After genetic analyses confirmed that the *NLRP3* mutation was causative, two of the affected members (subjects 1189 and 1236) and one of the unaffected carriers of the *NLRP3* mutation (subject 1238) in family LMG113 were reascertained at the NIH Clinical Center between 2013 and 2015, at which time they underwent another rheumatologic evaluation, a postcontrast MRI-FLAIR study of the temporal bones (including inner ears), and comprehensive serologic testing that included measurement of levels of CRP, fibrinogen, and ESR. PBMCs were collected for measurement of IL-1β secretion.

We ascertained the members of LMG446 at the NIH Clinical Center in 2015. The affected members (subjects 2261, 2262, 2264, and 2265) were evaluated as described above with medical history and physical examinations performed independently by neurotologists and rheumatologists, pure-tone and speech audiometry, MRI-FLAIR evaluation of the temporal bones, and comprehensive serologic testing. PBMCs from subjects 2262, 2264, and 2265 were collected for measurement of IL-1β secretion.

Imaging of the inner ear was performed on a 3.0-Tesla MRI (Achieva; Philips) system using a paradigm specifically designed to detect inner ear inflammation using high-resolution FLAIR sequences to suppress signal from the perilymph and endolymph. The data were obtained before and ≈25 min after intravenous injection of a single dose of 1 mmol/kg Gd-DTPA (Magnevist; Bayer). For each sequence, resolution was 0.3 × 0.3 × 1.8 mm, contrast parameters were a repetition time of 11,000 ms, inversion time of 2,550 ms, and an echo time of 120 ms, resulting in a scan time of 15 min. All images were reviewed by the same neuroradiologist (J.A.B.), neurotologist (H.J.K.), and otolaryngologist (A.J.G.).

Linkage Analysis. Genomic DNA was extracted from peripheral white blood cells (WBC) using standard procedures. We performed a genome-wide linkage analysis with 440 polymorphic STR markers that included markers closely linked to known DFNA and DFNB loci (33). In addition, we performed a genome-wide linkage scan with 6,090 SNPs on the Infinium HumanLinkage-12 Genotyping BeadChip (Illumina). Parametric LOD scores were calculated with the FastLink program on the easyLINKAGE Plus platform (54, 55). We designated the inheritance as autosomal dominant and the disease allele prevalence frequency as 0.001. Fine mapping was performed with STR markers and unannotated microsatellite markers. D1NIH10 amplification primer sequences were 5′-TTTTCTCCCTCCCCTGGTAT and 5′-TGAAATGAAT-TTCTATGAAATGAAGA. The two-point LOD score between DFNA34 and each marker was calculated with SuperLink software (56).

Mutation Analysis. We performed Sanger dideoxy nucleotide sequence analyses of PCR-amplified genes in the DFNA34 interval. PCR primers were designed to amplify all coding exons and their flanking sequences within the DFNA34 interval. Normal control chromosomes (572) were obtained from Coriell Cell Repositories (HD01-HD09, HD100CAU, and HD100CAU-2). Allele frequencies were derived from the ExAC browser (exac.broadinstitute.org).

Measurement of IL-1β in Culture Supernatants. PBMCs were isolated by Ficoll-Hypaque centrifugation of peripheral venous blood samples freshly drawn from subjects 1189, 1236, 1238, 2262, 2264, and 2265 in addition to healthy control subjects. Plastic-adherent PBMCs were cultured in RPMI supplemented with 10% FBS in 12-well culture plates (2 × 10⁶ cells per milliliter). Cells were treated with ultrapure LPS (1 μg/mL, from *Escherichia coli* 0127:B7; InvivoGen). After 3 h of treatment, cell culture media were replaced with

350 μL serum-free RPMI with or without 1 mM $CaCl_2$ for 60 min, and cell culture supernatants and cell lysates (with 100 μL lysis buffer) were collected. In some experiments, a small-molecule inhibitor (MCC950) of the NLRP3 inflammasome (57) was included to confirm the specificity of the observed responses. Ten microliters of lysate or 45 μL of cell culture supernatant was separated by SDS/PAGE for Western blotting with anti–IL-1β antibody (AF201NA; R&D Systems).

Animals. $Cx3cr1^{GFP}$ mice (JAX5582) in which the $Cx3cr1$ gene is replaced with the GFP reporter gene (37), $Nlrp3$ knockout ($Nlrp3^{\Delta}$) mice (JAX21302) in which the entire coding region of $Nlrp3$ is replaced with neomycin resistance gene (58), and C57BL/6J wild-type mice (JAX664) were purchased from the Jackson Laboratory to establish colonies in our animal facility. $Cx3cr1^{GFP}$ mice, on a mixed C57BL/6J; C57BL/6N genetic background, were crossed with wild-type C57BL/6J mice to generate $Cx3cr1^{GFP/+}$ mice.

Immunohistochemistry. Frozen sections (10-μm thick) of cochlea were prepared from $Cx3cr1^{GFP/+}$ mice as described previously (59). Sections were counterstained with Alexa Fluor 568 phalloidin (Life Technologies) diluted 1:500. Whole-mounted cochlear tissues from $Cx3cr1^{GFP/+}$ mice were immunostained with anti-CD34 or anti-F4/80 antibodies, as described previously (27, 28), with some modifications. Tissues were blocked with a solution of 5% goat serum and 2% BSA in PBS. Primary antibodies were Alexa Fluor 647-conjugated rat anti-CD34 (560230; BD Biosciences) or rat anti-F4/80 antibody (14-4801-85; eBioscience). The specimens were incubated with primary antibodies diluted 1:200 (for either primary antibody) in blocking solution, followed by incubation with secondary antibody (Alexa Fluor 568-conjugated goat anti-rat; Life technologies) diluted 1:500 for F4/80 staining. Sections or tissues were mounted with Prolong Gold Antifade with or without DAPI (Life Technologies) and visualized with an LMS 780 confocal microscope equipped with ZEN 2012 software (Carl Zeiss).

RT-PCR Analyses. Total RNA was extracted from the cochlea, brain, lung, or liver of C57BL/6J mice using the PicoPure RNA Isolation Kit (Life Technologies). Isolation of RNA from FACS-purified $Cx3cr1^{GFP}$ cells was performed using a ZYMO Quick-RNA Microprep kit (Zymo Corporation). RNA was reverse-transcribed using the SuperScript III First-Strand Synthesis System (Life Technologies). PCR primers were designed to amplify all of the coding regions of mouse $Nlrp3$, $Pycard$, $Casp1$, or $Il1b$ cDNA. Amplification products were verified by nucleotide sequence analysis.

For quantitative RT-PCR, we designed amplification primers specific to $Actb$, $Nlrp3$, $Pycard$, $Casp1$, $Il1b$, or $F4/80$ cDNA with a ZEN double-quenched probe containing a 5′ FAM fluorophore, a 3′ IBFQ quencher and an internal ZEN quencher (IDT) (Table S3). We used a premade set of primers and probe specific to $Cd45$ (Mm01293577_m1; Thermo Fisher Scientific). Comparative TaqMan assay was performed using TaqMan Fast Universal PCR Master Mix (Life Technologies) on a ViiA7 Real-Time PCR System (Life Technologies). Relative expression was normalized to the level of actin cytoplasmic 1 (encoded by $Actb$) and calculated using the comparative C_T method (60).

Isolation and Purification of $Cx3cr1^{GFP}$ Cochlear Cells. Mouse cochleae were harvested from seven P19 $Cx3cr1^{GFP}$ mice and one C57BL/6J mouse. Each of the specimens were microdissected in cold PBS to isolate the lateral wall of the cochlea and the spiral ganglion. Tissues were transferred to ice-cold PBS, excess supernatant was removed, and 0.05% trypsin was applied during an incubation at 37 °C for 8 min. The trypsin solution was removed and specimens were triturated in 5% FBS with a 200- or 1,000-μL pipette for 2 min in a total volume of 600–700 μL. The pooled lateral wall and spiral ganglion cell suspensions were filtered with a 40-μm nylon mesh. Samples from each strain were transferred to a polystyrene tube (on ice) and resuspended in 5% FBS (600 μL total volume). Cells were kept on ice until RNA preparation, except during FACS. To assess cell viability and prevent inclusion of dead cells or debris in samples collected during FACS, cells from C57BL/6J and $Cx3cr1^{GFP/GFP}$ mice were isolated and labeled with propidium iodide (Life Technologies) before initiation of FACS. Cell collection and separation was performed using a FACSAria III flow cytometer (BD Biosciences) with 488-nm excitation and a 100-μm nozzle. Gating parameters were optimized using both C57BL/6J and $Cx3cr1^{GFP/GFP}$ samples to collect healthy cells with either low (<200) or high (>1,000) GFP signal intensities. Each respective cell population was collected in 20% FBS solution and placed on ice.

Measurement of IL-1β in Mouse Cochlear Culture Supernatant. Mouse cochleae were harvested from four P3–P4 C57BL/6J or $Nlrp3^{\Delta/\Delta}$ mice and placed in ice-cold Leibovitz's L-15 Medium (Life Technologies) under sterile conditions. Each cochlea was microdissected into organ of Corti, lateral wall, and auditory nerve portions. After a 10-min wash in ice-cold medium, the cochlear portions from the four mice were incubated with humidification in DMEM/Nutrient Mixture F12 supplemented with 10% FBS (Life Technologies) and 100 μg/mL ampicillin (Sigma-Aldrich) at 37 °C and 5% CO_2. Different tissue culture plates were used depending on the volume of culture medium: 12-well tissue culture plates (3.8-cm² culture surface per well; Sigma-Aldrich) were used for 1.0-mL volumes and 24-well tissue culture plates (1.9-cm²; Sigma-Aldrich) were used for 0.4-mL volumes. Three different culture paradigms were used. In the first condition, tissues were incubated for 20 h without stimulation. In the second condition, tissues were incubated for 3 h, followed by the stimulation with 1 μg/mL LPS (from *E. coli* 0111:B4; Sigma-Aldrich) for 17 h. In the third condition, tissues were incubated for 3 h and then stimulated with 1 μg/mL LPS for 16 h, followed by stimulation with LPS and 5 mM ATP (Sigma-Aldrich) for 1 h. After 20 h of incubation under any of the three conditions, the culture supernatant was collected and stored at −80 °C. IL-1β concentration was measured using the Mouse IL-1β Quantikine ELISA KIT (R&D systems). Cultured cochlear tissues were also harvested for quantitative RT-PCR analysis. For each culture condition, three independent biological replicates were performed, and the averaged IL-1β concentrations and RNA levels were shown.

Immunohistochemistry of Cultured Cochlea. Cochleae were harvested from P4 $Cx3cr1^{GFP/+}$ mice and microdissected into organ of Corti and lateral wall portions. Each tissue sample was placed on a 3.5-mm tissue culture dish (Sigma-Aldrich) coated with Cell-Tak Cell and Tissue Adhesive (Fisher Scientific). Tissues were incubated in 2 mL culture medium for 20 h using two of the three different conditions described above: no stimulation for the entire 20 h or no stimulation for 3 h followed by stimulation with LPS for 17 h. After incubation, the samples were fixed in 4% paraformaldehyde in PBS for 30 min at room temperature. After a 30-min permeabilization with 0.1% saponin (Sigma-Aldrich), tissues were blocked with 5% normal donkey serum with 0.05% saponin for 1 h. They were incubated with a goat anti–IL-1β antibody (AF-401-NA; R&D Systems) at 1:50 dilution in the blocking solution overnight at 4 °C. Following five washes with 0.05% saponin, samples were incubated with a donkey anti-goat IgG antibody conjugated to Alexa Fluor 568 (Life Technologies) at 1:500 dilution in blocking solution for 1 h at room temperature. After five washes with 0.05% saponin, tissues were mounted and visualized by confocal microscopy.

Statistics. Statistical analyses included Student's *t* test and one-way ANOVA. $P < 0.05$ was considered to be significant.

Study Approval. This study was approved by the Combined Neurosciences Institutional Review Board of the National Institutes of Health in Bethesda, Maryland. Written informed consent was obtained from adult subjects and from the parent or legal guardian of minor subjects. Rheumatologic evaluations and anakinra administration were performed with informed consent as part of either of two studies approved by the Institutional Review Board of the National Human Genome Research Institute or the joint Institutional Review Board of the National Institute of Arthritis and Musculoskeletal and Skin Diseases and the National Institute of Diabetes and Digestive and Kidney Diseases, respectively. All animal experiments and procedures adhered to protocols approved by the joint Animal Care and Use Committee of the National Institute of Neurological Disorders and Stroke and the National Institute on Deafness and Other Communication Disorders.

1. Agostini L, et al. (2004) NALP3 forms an IL-1beta-processing inflammasome with increased activity in Muckle-Wells autoinflammatory disorder. *Immunity* 20:319–325.
2. Gross O, et al. (2012) Inflammasome activators induce interleukin-1α secretion via distinct pathways with differential requirement for the protease function of caspase-1. *Immunity* 36:388–400.
3. Guarda G, et al. (2011) Differential expression of NLRP3 among hematopoietic cells. *J Immunol* 186:2529–2534.
4. Sutterwala FS, et al. (2006) Critical role for NALP3/CIAS1/cryopyrin in innate and adaptive immunity through its regulation of caspase-1. *Immunity* 24: 317–327.

5. Hoffman HM, Mueller JL, Broide DH, Wanderer AA, Kolodner RD (2001) Mutation of a new gene encoding a putative pyrin-like protein causes familial cold auto-inflammatory syndrome and Muckle-Wells syndrome. *Nat Genet* 29:301–305.

6. Mariathasan S, et al. (2004) Differential activation of the inflammasome by caspase-1 adaptors ASC and Ipaf. *Nature* 430:213–218.

7. Martinon F, Burns K, Tschopp J (2002) The inflammasome: A molecular platform triggering activation of inflammatory caspases and processing of proIL-beta. *Mol Cell* 10:417–426.

8. Sutterwala FS, Haasken S, Cassel SL (2014) Mechanism of NLRP3 inflammasome activation. *Ann N Y Acad Sci* 1319:82–95.

9. Horvath GL, Schrum JE, De Nardo CM, Latz E (2011) Intracellular sensing of microbes and danger signals by the inflammasomes. *Immunol Rev* 243:119–135.

10. Lee GS, et al. (2012) The calcium-sensing receptor regulates the NLRP3 inflammasome through Ca2+ and cAMP. *Nature* 492:123–127.

11. Ahmadi N, et al. (2011) Cryopyrin-associated periodic syndromes: Otolaryngologic and audiologic manifestations. *Otolaryngol Head Neck Surg* 145:295–302.

12. Jesus AA, Goldbach-Mansky R (2014) IL-1 blockade in autoinflammatory syndromes. *Annu Rev Med* 65:223–244.

13. Chen P, et al. (2016) NLRP3 is expressed in the spiral ganglion neurons and associated with both syndromic and nonsyndromic sensorineural deafness. *Neural Plast* 2016: 3018132.

14. Aksentijevich I, et al. (2002) De novo CIAS1 mutations, cytokine activation, and evidence for genetic heterogeneity in patients with neonatal-onset multisystem inflammatory disease (NOMID): A new member of the expanding family of pyrin-associated auto-inflammatory diseases. *Arthritis Rheum* 46:3340–3348.

15. Feldmann J, et al. (2002) Chronic infantile neurological cutaneous and articular syndrome is caused by mutations in CIAS1, a gene highly expressed in polymorpho-nuclear cells and chondrocytes. *Am J Hum Genet* 71:198–203.

16. Goldbach-Mansky R, et al. (2006) Neonatal-onset multisystem inflammatory disease responsive to interleukin-1beta inhibition. *N Engl J Med* 355:581–592.

17. Hoffman HM, et al. (2004) Prevention of cold-associated acute inflammation in familial cold autoinflammatory syndrome by interleukin-1 receptor antagonist. *Lancet* 364:1779–1785.

18. Kuemmerle-Deschner JB, et al. (2011) Efficacy and safety of anakinra therapy in pediatric and adult patients with the autoinflammatory Muckle-Wells syndrome. *Arthritis Rheum* 63:840–849.

19. Conforti-Andreoni C, Ricciardi-Castagnoli P, Mortellaro A (2011) The inflammasomes in health and disease: From genetics to molecular mechanisms of autoinflammation and beyond. *Cell Mol Immunol* 8:135–145.

20. Masters SL, Simon A, Aksentijevich I, Kastner DL (2009) Horror autoinflammaticus: The molecular pathophysiology of autoinflammatory disease (*). *Annu Rev Immunol* 27: 621–668.

21. Sibley CH, et al. (2012) Sustained response and prevention of damage progression in patients with neonatal-onset multisystem inflammatory disease treated with ana-kinra: A cohort study to determine three- and five-year outcomes. *Arthritis Rheum* 64: 2375–2386.

22. de Koning HD, et al. (2015) Myeloid lineage-restricted somatic mosaicism of NLRP3 mutations in patients with variant Schnitzler syndrome. *J Allergy Clin Immunol* 135:561–564.

23. Nakagawa K, et al. (2015) Somatic NLRP3 mosaicism in Muckle-Wells syndrome. A genetic mechanism shared by different phenotypes of cryopyrin-associated periodic syndromes. *Ann Rheum Dis* 74:603–610.

24. Tanaka N, et al. (2011) High incidence of NLRP3 somatic mosaicism in patients with chronic infantile neurologic, cutaneous, articular syndrome: Results of an International Multicenter Collaborative Study. *Arthritis Rheum* 63:3625–3632.

25. Hirose K, Discolo CM, Keasler JR, Ransohoff R (2005) Mononuclear phagocytes migrate into the murine cochlea after acoustic trauma. *J Comp Neurol* 489:180–194.

26. Shi X (2010) Resident macrophages in the cochlear blood-labyrinth barrier and their renewal via migration of bone-marrow-derived cells. *Cell Tissue Res* 342:21–30.

27. Zhang W, et al. (2012) Perivascular-resident macrophage-like melanocytes in the inner ear are essential for the integrity of the intrastrial fluid-blood barrier. *Proc Natl Acad Sci USA* 109:10388–10393.

28. Ito T, et al. (2014) Slc26a4-insufficiency causes fluctuating hearing loss and stria vascularis dysfunction. *Neurobiol Dis* 66:53–65.

29. Bonar SL, et al. (2012) Constitutively activated NLRP3 inflammasome causes inflammation and abnormal skeletal development in mice. *PLoS One* 7:e35979.

30. Brydges SD, et al. (2009) Inflammasome-mediated disease animal models reveal roles for innate but not adaptive immunity. *Immunity* 30:875–887.

31. Meng G, Zhang F, Fuss I, Kitani A, Strober W (2009) A mutation in the Nlrp3 gene causing inflammasome hyperactivation potentiates Th17 cell-dominant immune responses. *Immunity* 30:860–874.

32. Steel KP, Bock GR (1980) The nature of inherited deafness in deafness mice. *Nature* 288:159–161.

33. Kurima K, et al. (2000) Genetic map localization of DFNA34 and DFNA36, two autosomal dominant non-syndromic deafness loci. *Am J Hum Genet* 67:300.

34. Csak T, et al. (2011) Fatty acid and endotoxin activate inflammasomes in mouse hepatocytes that release danger signals to stimulate immune cells. *Hepatology* 54: 133–144.

35. Halle A, et al. (2008) The NALP3 inflammasome is involved in the innate immune response to amyloid-beta. *Nat Immunol* 9:857–865.

36. Tran HB, et al. (2012) Immunolocalization of NLRP3 inflammasome in normal murine airway epithelium and changes following induction of ovalbumin-induced airway inflammation. *J Allergy (Cairo)* 2012:819176.

37. Jung S, et al. (2000) Analysis of fractalkine receptor CX(3)CR1 function by targeted deletion and green fluorescent protein reporter gene insertion. *Mol Cell Biol* 20: 4106–4114.

38. Austyn JM, Gordon S (1981) F4/80, a monoclonal antibody directed specifically against the mouse macrophage. *Eur J Immunol* 11:805–815.

39. Rabinowitz SS, Gordon S (1991) Macrosialin, a macrophage-restricted membrane sialoprotein differentially glycosylated in response to inflammatory stimuli. *J Exp Med* 174:827–836.

40. Mariathasan S, et al. (2006) Cryopyrin activates the inflammasome in response to toxins and ATP. *Nature* 440:228–232.

41. Compeyrot-Lacassagne S, Tran TA, Guillaume-Czitrom S, Marie I, Koné-Paut I (2009) Brain multiple sclerosis-like lesions in a patient with Muckle-Wells syndrome. *Rheumatology (Oxford)* 48:1618–1619.

42. Lequerré T, et al. (2007) A cryopyrin-associated periodic syndrome with joint destruction. *Rheumatology (Oxford)* 46:709–714.

43. Gris D, et al. (2010) NLRP3 plays a critical role in the development of experimental autoimmune encephalomyelitis by mediating Th1 and Th17 responses. *J Immunol* 185:974–981.

44. Neven B, et al. (2010) Long-term efficacy of the interleukin-1 receptor antagonist anakinra in ten patients with neonatal-onset multisystem inflammatory disease/chronic infantile neurologic, cutaneous, articular syndrome. *Arthritis Rheum* 62: 258–267.

45. Gomez Perdiguero E, et al. (2015) Tissue-resident macrophages originate from yolk-sac-derived erythro-myeloid progenitors. *Nature* 518:547–551.

46. Murray PJ, Wynn TA (2011) Protective and pathogenic functions of macrophage subsets. *Nat Rev Immunol* 11:723–737.

47. Sato E, Shick HE, Ransohoff RM, Hirose K (2008) Repopulation of cochlear macrophages in murine hematopoietic progenitor cell chimeras: The role of CX3CR1. *J Comp Neurol* 506:930–942.

48. Vambutas A, et al. (2014) Early efficacy trial of anakinra in corticosteroid-resistant autoimmune inner ear disease. *J Clin Invest* 124:4115–4122.

49. Hu C, et al. (2015) NLRP3 deficiency protects from type 1 diabetes through the regulation of chemotaxis into the pancreatic islets. *Proc Natl Acad Sci USA* 112: 11318–11323.

50. Yamasoba T, et al. (2013) Current concepts in age-related hearing loss: Epidemiology and mechanistic pathways. *Hear Res* 303:30–38.

51. Zhou R, Yazdi AS, Menu P, Tschopp J (2011) A role for mitochondria in NLRP3 inflammasome activation. *Nature* 469:221–225.

52. International Organization for Standardization (2000) Acoustics–Statistical distribution of hearing thresholds as a function of age. ISO 7029 (International Organization for Standardization, Geneva).

53. Clark JG (1981) Uses and abuses of hearing loss classification. *ASHA* 23:493–500.

54. Cottingham RW, Jr, Idury RM, Schäffer AA (1993) Faster sequential genetic linkage computations. *Am J Hum Genet* 53:252–263.

55. Hoffmann K, Lindner TH (2005) easyLINKAGE-Plus—Automated linkage analyses using large-scale SNP data. *Bioinformatics* 21:3565–3567.

56. Fishelson M, Geiger D (2002) Exact genetic linkage computations for general pedigrees. *Bioinformatics* 18(Suppl 1):S189–S198.

57. Coll RC, et al. (2015) A small-molecule inhibitor of the NLRP3 inflammasome for the treatment of inflammatory diseases. *Nat Med* 21:248–255.

58. Kovarova M, et al. (2012) NLRP1-dependent pyroptosis leads to acute lung injury and morbidity in mice. *J Immunol* 189:2006–2016.

59. Hertzano R, et al. (2011) Cell type-specific transcriptome analysis reveals a major role for Zeb1 and miR-200b in mouse inner ear morphogenesis. *PLoS Genet* 7:e1002309.

60. Kurima K, et al. (2011) A noncoding point mutation of Zeb1 causes multiple developmental malformations and obesity in Twirler mice. *PLoS Genet* 7:e1002307.